IOP Conf. Series: Materials Science and Engineering **101** (2015) 012191 doi:10.1088/1757-899X/101/1/012191

15 K liquid hydrogen thermal Energy Storage Unit for future ESA science missions

P Borges de Sousa[1], D Martins[2], G Tomás[1], J Barreto[1], J Noite[2], M Linder[3], D Fruchart[4], P de Rango[4], R Haettel[4], I Catarino[1] and G Bonfait[1]

[1] LIBPhys, Physics Department, Faculty of Sciences and Technology, Universidade Nova de Lisboa, 2829-516 Caparica, Portugal
[2] Active Space Technologies, Parque Industrial de Taveiro, Lote 12, 3045-508 Coimbra, Portugal
[3] European Space Agency, ESTEC, E0053A, 2200 AG Noordwijk, The Netherlands
[4] CNRS, Institut Néel et CRETA, F-38000 Grenoble, France

E-mail: p.sousa@campus.fct.unl.pt

Abstract. A thermal Energy Storage Unit (ESU) using liquid hydrogen has been developed as a solution for absorbing the heat peaks released by the recycling phase of a 300 mK cooler that is a part of the cryogenic chain of one of ESA's new satellites for science missions. This device is capable of storing 400 J of thermal energy between 15 and 16 K by taking advantage of the liquid-to-vapor latent heat of hydrogen in a closed system. This paper describes some results obtained with the development model of the ESU under different configurations and using two types of hydrogen storage: a large expansion volume for ground testing and a much more compact unit, suitable for space applications and that can comply with ESA's mass budget.

1. Introduction

ESA has selected ATHENA (the Advanced Telescope for High-Energy Astrophysics) as its second large-class science mission, designed to study the hot and energetic universe: its launch is foreseen to take place in 2028. One of the instruments that will compose ATHENA is the X-ray Integral Field Unit (X-IFU), which is an advanced X-ray microcalorimeter spectrometer composed of an array of transition-edge sensors (TES). The detector array must be cooled down to temperatures below 100 mK: for this reason, a complex cryogenic chain must be developed for the X-IFU instrument, able to cool the sensor from 300 K to around 50 mK. Since this mission should be able to run for 10 years, a cryogenic chain that doesn't rely on open-system cryogenic baths should be used.

In this cryochain, the regeneration of a sorption cooler will be responsible for releasing a heat burst of around 400 J (with a duration of 30 min) every 24 hours on a Joule-Thomson cooler working at 15 K [1]. This additional heat load can compromise the performance of the J-T's 15 K stage, as the coolers might not be able to maintain the stage's temperature. The requirements are that the 15 K stage temperature does not rise above 16 K for a period longer than 10 minutes during the 30 min, 400 J heat load.

As a solution, we propose using a thermal Energy Storage Unit (ESU) that is able to temporarily store these 400 J without a large temperature increase (from 15 K to 16 K) during the

30 min heat burst, hence avoiding a large thermal load on the 15 K stage. In order to minimize both volume and mass in the low temperature part of the cryogenic chain, this solution takes advantage of the relatively high latent heat of the liquid-to-vapor transition of hydrogen in a closed system when compared to that of a solid-liquid phase change [2] or to the sensible heat of solid materials [3].

The 400 J coming from the sorption cooler cause the liquid hydrogen inside the cell to evaporate (thermal energy absorption phase, called "ESU mode"); because this happens in a closed system, the evaporation will cause the pressure to increase, which in turn will cause the temperature to increase (the phase change occurs along the liquid-vapor saturation curve). To avoid a large temperature increase, the resulting hydrogen gas needs to be stored at a pressure close to the saturation pressure at 15 K. This can either be achieved by having a large expansion volume [4] or by using more compact storage methods. After the heat burst has been absorbed, the ESU is cooled again to its base temperature of 15 K and hydrogen is re-condensed inside the cell over the next 24 hours, ready for a new cycle. This type of device has been thoroughly tested in our laboratory using different fluids [4, 5] or solid materials [3] for different temperature ranges.

2. System description

The system's overall schematic is shown in figure 1. It is divided into three parts, according to their main functions: a room temperature hydrogen storage vessel, intermediate interfaces used for gas pre-cooling and the cold part, comprised mainly by the liquid hydrogen cell which is directly coupled to the heat burst source.

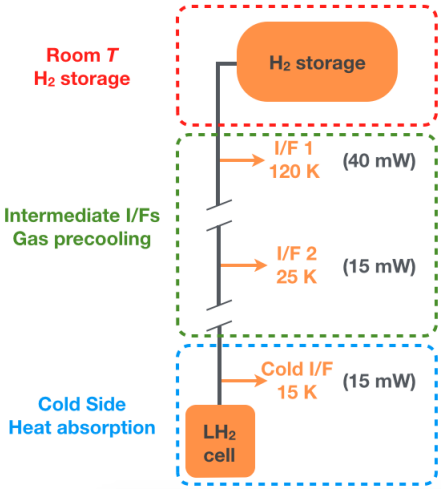

Figure 1. Overall schematic of the ESU and its three main components: the room temperature gas storage, the intermediate interfaces for gas pre-cooling, and the cold cell where the heat load is absorbed. The available cooling power (cf. ESA requirements) is indicated for each of the interfaces.

2.1. Room temperature storage

The room temperature part has the function of storing all the hydrogen gas that is evaporated during the ESU mode: this gas must be stored at low pressure between 125 and 200 mbars, which is the range of saturation pressure that corresponds to 15−16 K. The choice of storage depends heavily on the purpose of the system: a large expansion volume may be suitable for ground testing, but impracticable for a compact and light system designed for space. For testing the various configurations and capabilities of the low temperature cell, as well as for verifying the compliance of the system with ESA's requirements, expansion volumes of 6 and 56 liters were used. Then a more compact solution was implemented, using metal hydrides to absorb hydrogen during the ESU mode: this solution allows for the 400 J to be stored with a temperature

rise above 16 K for less than 10 min, whereas that would only be achievable with an ordinary expansion volume larger than 100 liters. It also allows us to comply with the given mass/volume budget, making this solution a viable one for space missions.

For the expansion volume, the size is mainly defined by the maximum allowed pressure increase, which in turn sets the maximum temperature rise in the cold cell during the evaporation phase. Table 1 compares the necessary volume needed to maintain different temperature drifts during the ESU mode and shows that maintaining a temperature below 16.5 K requires expansion volumes that are hardly compatible with the requirements for space missions.

Table 1. Expansion volume requirements for different cold cell temperature drifts. Data for expansion volumes at room temperature, and for a energy storage in the cold cell of 400 J, computed using the model described in [4].

Room T volume	Filling pressure	T rise in the cold cell
100 ℓ	0.240 bar	From 15 to 16.3 K
50 ℓ	0.345 bar	From 15 to 17.2 K
10 ℓ	1.170 bars	From 15 to 20.8 K
6 ℓ	1.800 bars	From 15 to 22.3 K

A metal hydride-filled canister was chosen as a viable solution due to its capacity to store hydrogen in a much more compact way, compatible with the constraints imposed by working in a space environment. The metal hydride $LaNi_{4.8}Sn_{0.2}$ was selected for its special properties [6]: this particular alloy of the $LaNi_5$ family enables the material to absorb hydrogen at low pressures at room temperature (in the range of 100−300 mbars). Tin also has a role in dramatically decreasing degradation and improving the stability of the hydride [7]. This material was studied and used to integrate a hydrogen compressor for the Planck mission [8].

The $LaNi_{4.8}Sn_{0.2}$ material used in this work was developed at CNRS/Inst. Néel. High-purity lanthanum, nickel and tin were used for the preparation of several ingots which were then annealed for further homogenization. The ingots were then ground together into coarse chunks and activated with a high pressure of pure hydrogen, which turned them into a ≈ 14 μm powder. The canister itself consists of a 360 cm^3 316 stainless steel vessel, connected to a 4 W @ 273 K cooling source to manage the heat of absorption released by the metal hydride during the ESU mode. Inside the canister, which was largely inspired on the work of Bowman Jr. [6], the metal hydride powder fills an aluminum foam (93% porosity) that enhances the heat transfer between the metal hydride and the canister walls, while providing structural support to the powdered metal.

2.2. Intermediate interfaces

Two radiation shields are foreseen for the cryogenic chain, at 120 K (I/F 1) and 25 K (I/F 2). We can take advantage of the available cooling power at each stage by thermally coupling the capillary that runs from the cold cell to the room temperature part to these stages. This is fundamental for pre-cooling the gas as it is coming from the room temperature storage part before it reaches the cell and condenses, as well as reducing parasitic heat loads arriving through solid conduction from the capillary itself.

2.3. Cold cell

The low temperature cell is thermally coupled to the source of the heat bursts, which will release 400 J according to a specific Heat Load Profile (HLP) shown in the next section. It is

composed by a cylindrical copper reservoir filled with alumina foam, with a free void volume of 15.6 cm^3. This foam is a highly porous ceramic ($\approx$ 91% free volume) with a mean pore size lower than 250 μm, and is used to confine liquid hydrogen inside the cell through capillary action, regardless of the direction of gravity acceleration. The use of porous materials is a key element in space applications that require the use of liquids, since microgravity environments call for other solutions for liquid confinement.

The cell has two flat mounts for thermal coupling of the heaters and the cooling source, as well as thermometers, and two capillary exhausts: one that connects it to the room temperature storage and where the hydrogen gas flows during operation, and a second capillary connected to a room temperature pressure sensor for measurements free of pressure drop. The cell can be mounted so that the exhaust capillary is either at the top of the cell, which we call the "baseline configuration", or at its bottom, in the "antigravity configuration", to test liquid confinement. In the latter configuration, if the foam does not confine the liquid, it would accumulate at the bottom and be spilled out as soon as the pressure inside the cell increases during the ESU mode.

3. Results and discussion

3.1. Baseline vs. anti-gravity configuration

To assess whether the alumina foam was able to confine the liquid hydrogen inside the cell and to verify that the cell was able to store 400 J, hydrogen was condensed inside the cell up to a 90% liquid filling ratio and ESU mode experiments were performed by applying a constant heat load to the cell. The cell was first tested in its baseline configuration, where the capillary exhaust is at the top of the cell and hence no spilling can occur. Then, tests were performed in its anti-gravity configuration, where the exhaust is located at the bottom of the cell. Figure 2 shows the results for the temperature drifts in the cell during ESU modes performed in both configurations.

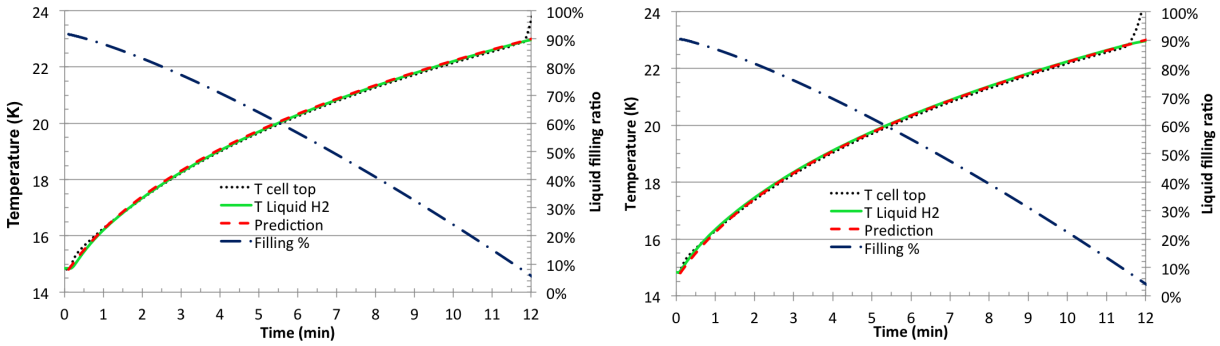

(a) Baseline configuration. (b) Anti-gravity configuration.

Figure 2. ESU modes in the two configurations. At $t = 0$ a constant heat load of 0.7 W is applied. Full (——) lines represent the temperature inside the cell deduced from the saturation pressure measured at room temperature, dotted (· · · · · ·) lines the temperature of the cell walls, dashed (- - - -) lines the temperature predicted by our thermodynamic model and chain (— · —) lines the amount of liquid in the cell (to be read in the right-hand side axis).

The results shown above were obtained with a 6-liter expansion volume and with a constant heat load of 0.7 W applied to the cell walls. There is no observable difference between the two experiments, of which we conclude that the alumina foam effectively retains all of the liquid hydrogen inside the cell, even with an applied heat load that can generate temperature differences and gas flow inside the cell, which could potentially disturb the capillary effects. The

results also show a good agreement between the temperatures measured by the thermometers in the cell and the one computed from pressure measurements, $T_{liquidH_2}$, that measures the liquid-vapor interface temperature inside the cell: this shows that the cell does not need to be designed to have heat exchangers on its inside.

In the experiments with the 6-liter expansion volume, the cell is able to absorb heat during $\approx$ 11.5 min by hydrogen evaporation (a total of 480 J was stored) within a temperature drift of $\approx$ 8 K. These experimental results are in very good agreement with thermodynamical calculations [3], as shown by the nearly perfect matching of the experimental data and the temperature drift calculated using this model.

3.2. Metal hydride isotherms

The previously described canister was filled with the $LaNi_{4.8}Sn_{0.2}$ powder. The canister was then connected to the low temperature cell, replacing the expansion volume. Before operation, a small sample of the powder was taken for pressure-composition-temperature analysis (PCT), in order to verify compliance with our requirements. These measurements were carried out by the CNRS team after synthesizing the material. Figure 3 shows the results for three selected temperatures within our range of interest. The x-axis represents the mean number of hydrogen atoms absorbed into one molecule of $LaNi_{4.8}Sn_{0.2}$, and the fairly flat plateaus of the curves denote the progressive absorption of hydrogen thanks to La−H chemical bonds. When a $LaNi_{4.8}Sn_{0.2}H_5$ molecule is formed, no more chemical bonds are available and further absorption needs very high pressures to be achieved.

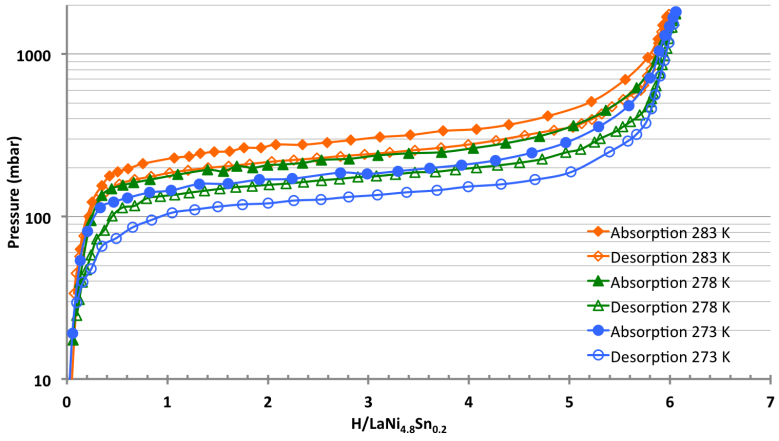

Figure 3. PCT curves for the $LaNi_{4.8}Sn_{0.2}$ powder synthesized at CNRS/Inst. Néel and used for hydrogen gas storage.

The results obtained by CNRS/Inst. Néel are similar to those obtained by Bowman Jr. [6]. However, while the plateaus are flat for a large range of $H/LaNi_{4.8}Sn_{0.2}$ in his results (*e.g.*, in the 273 K isotherm, pressure remains at around 100 mbars throughout the whole absorption range, from 1 to 5 $H/LaNi_{4.8}Sn_{0.2}$), our results show a slight increase in pressure as the amount of absorbed hydrogen increases: at 273 K, for 1 $H/LaNi_{4.8}Sn_{0.2}$ we have an equilibrium pressure of 145 mbars, while for 5 $H/LaNi_{4.8}Sn_{0.2}$ it is 284 mbars. This issue is still under study.

3.3. Expansion volume vs. metal hydride experiments

Both ESU mode experiments shown in figs. 4 and 5 were performed with the low temperature cell in its "antigravity configuration", *i.e.* with the capillary exhaust on the bottom of the

cell, which is considered the "worst-case scenario". Two thermometers are placed at each end of the low temperature cell, and a third temperature ($T_{liquidH_2}$) was computed from pressure measurements at room temperature as was previously mentioned. In these experiments, the heat load applied to the low temperature cell varies with time (dotted line in figs. 4 and 5, right-hand side axis) to mimic the heat released during the regeneration phase of the the sorption cooler [1]: the total duration of the Heat Load Profile (HLP) is 30 min. Figure 4 shows the results obtained in the case where the low temperature cell is connected to a 56-liter volume.

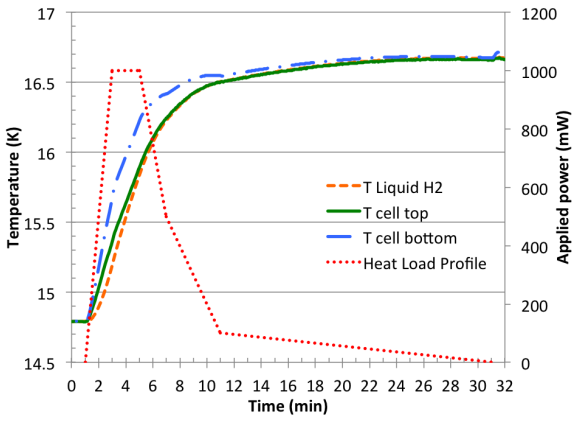

Figure 4. HLP applied to the low T cell with a 56-liter expansion volume for gas storage.

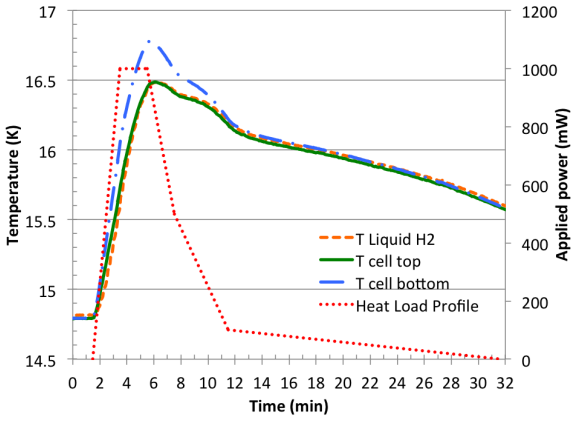

Figure 5. HLP applied to the low T cell with the $LaNi_{4.8}Sn_{0.2}$ canister as the gas storage unit.

With the 56-liter expansion volume, the pressure (and hence the temperature) inside the system progressively increase, as the hydrogen is evaporated and stored in the expansion volume as gas (cf. figure 4): 400 J were stored with a temperature drift of 3 K, with the maximum temperature throughout the HLP being 16.7 K at the end of the heat load.

When using the metal hydride canister (figure 5), during the HLP the cell reaches a maximum of 16.8 K (on the side it is being heated), and is at a temperature higher than 16 K for less than 12 minutes, quickly recovering from this temperature increase after the initial heating. This is compliant with ESA requirements for the maximum allowed temperature increase for the cell. During this period, temperature increases inside the cell due to the pressure that initially builds up as the canister temperature increases from $t = 2$ to $t = 6$ min (from 273 K up to 280 K, not shown): during this phase, absorption is performed at a higher pressure than expected for two reasons. One is the limited dynamics of hydrogen absorption by $LaNi_{4.8}Sn_{0.2}$: the evaporation rate can be higher than the absorption rate leading to a pressure increase, making it higher than that of the PCT equilibrium curve. The second one is due to the temperature increase of the $LaNi_{4.8}Sn_{0.2}$ powder due to the heat of absorption released (32 kJ/mole). For example, this heat rate can be evaluated to 35 W when 1 W is applied to the cell (evaporation rate $\approx 1 \times 10^{-3}$ moles/s), much higher than the cooling power available for the canister, which is $\approx$ 5 W at 0 °C. As can be seen in figure 3 this temperature increase leads to an increase of the equilibrium pressure in the system and hence to a temperature drift of the low temperature cell. During the rest of the HLP (from $t = 6$ to $t = 32$ min), temperatures measured in the low temperature cell start to decrease again, drifting back to $\approx$ 15.6 K at the end of the cycle. This happens because the heat load applied on the cell decreases, causing the evaporation rate to decrease as well: the absorption rate is now higher than the evaporation rate, and the canister can absorb all of the incoming hydrogen without increasing its temperature (meaning that the $\approx$ 5 W at 0 °C cooling power is now enough to cope with the released heat of absorption).

Beyond their relative compactness, these results show that this $LaNi_{4.8}Sn_{0.2}$ canister solution is preferable to the 56-liter volume solution, as the low temperature cell exceeds 16 K during a shorter period of time, avoiding an extra heat load to the 15 K stage and/or a degradation of the J-T cooling performance.

4. Conclusions

A solution for absorbing sporadic heat bursts that could otherwise severely disturb a cryogenic chain in the ATHENA satellite is presented. Our device is able to store more than 400 J of thermal energy, while keeping a light and compact cold cell at temperatures between 15 and 16 K, thus dramatically improving the stability of the system. This solution enables heat bursts to be managed without the use of large liquid reservoirs or over dimensioning some elements of the cryogenic chain, making it a suitable device for space applications. We have described some of the mandatory precautions that need to be taken into account to make it compliant with space systems, such as managing micro-gravity, and building a sturdy and compact system, especially on the hydrogen gas storage unit. Results show good compliance with the requirements given by ESA at the Development Model stage. More thorough and descriptive results will be obtained with the Engineering Model, which is beyond of the scope of this paper.

Acknowledgements

This work was supported by the European Space Agency (ESTEC contract 4000108532/NL/E) and partially supported by Fundação para a Ciência e Tecnologia (PEst-OE/FIS/UI0068/2014 and PTDC/EME-MFE/101448/2008). We also greatly acknowledge R. C. Bowman Jr. for sharing information about the LaNiSn compounds and for interesting and useful discussions.

References

[1] Duband L, Clerc L, Ercolani E, Guillemet L and Vallcorba R 2008 *Cryogenics* **48** 95 – 105
[2] Charles I, Coynel A and Daniel C 2008 *Proceedings of the 16th International Cryocooler Conference*
[3] Afonso J, Catarino I, Martins D, Ricardo J, Patricio R, Duband L and Bonfait G 2010 *Cryogenics* **50** 522 – 528 2009 Space Cryogenic Workshop
[4] Afonso J, Catarino I, Patrício R, Rocaboy A, Linder M and Bonfait G 2011 *Cryogenics* **51** 621 – 629
[5] Martins D, Borges de Sousa P, Catarino I and Bonfait G 2015 *Physics Procedia* **67** 1193 – 1198 proceedings of the 25th International Cryogenic Engineering Conference and International Cryogenic Materials Conference 2014
[6] Bowman Jr R 2003 *Journal of Alloys and Compounds* **356–357** 789 – 793 proceedings of the Eighth International Symposium on Metal-Hydrogen Systems, Fundamentals and Applications (MH2002)
[7] Bowman Jr R, Luo C, Ahn C, Witham C and Fultz B 1995 *Journal of Alloys and Compounds* **217** 185 – 192
[8] Morgante G, Barber D, Bhandari P, Bowman R C, Cowgill P, Crumb D, Loc T, Nash A, Pearson D, Prina M, Sirbi A, Schemlzel M, Sugimura R and Wade L A 2002 *AIP Conference Proceedings* **616** 298–302